

PROGRESSIVE COLLAPSE OF ISOLATED BUILDING SUBJECTED TO MULTI-HAZARD LOADING

Yongfeng DU

Professor, Institute of Earthquake Protection and Disaster Mitigation, Lanzhou University of Technology, Lanzhou, China
dooyf@lut.cn

Xiaohong ZENG Hu LI Haocai DUAN Qingxin ZHU

Graduate students, Institute of Earthquake Protection and Disaster Mitigation, Lanzhou Univ. of Technology, Lanzhou, China
892500912@qq.com

Keywords: isolated structure ; blast load ; progressive collapse ; fluid-structure interaction

1. Objectives

Isolation structure can effectively reduce the horizontal earthquake input to the super-structure by introducing the rubber bearing between foundation and the super-structure. Many isolated structures experienced the recent major earthquakes occurred in different part of the world, and the effectiveness of isolation technique in mitigating structural damage and protecting the equipments inside the building are widely recognized. Successively occurred earthquakes, on the other hand, enhanced people's desire of using new technology, such as isolation, for structure seismic protection in earthquake prone area. However, as the number of isolation applications in the world become more and more, the concern of progressive collapse of isolated structure subjected to multi hazard such as the blast loading, earthquake, and uneven settlement of collapsible loess on the base isolated structures.

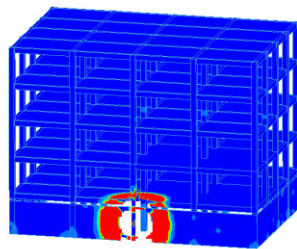
2. Relevant Results

Based on the direct simulation method, the interaction between the structure and the blast wave in the basement of the isolated structure is simulated and analyzed. The failure mode of the isolated structure after the explosion in the basement is discussed.

Explosive shockwave expression satisfies one dimensional unsteady flow equations:

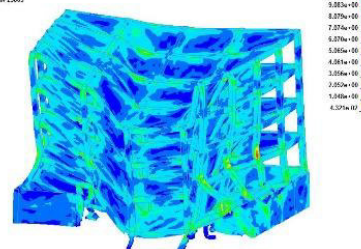
$$\begin{aligned}
 A \frac{\partial \rho}{\partial t} + \frac{\partial(A\rho u)}{\partial x} &= 0 \\
 \frac{\partial u}{\partial t} + u \frac{\partial u}{\partial x} + \frac{1}{\rho} \frac{\partial P}{\partial x} &= 0 \\
 \frac{de}{dt} + \frac{P}{A\rho} \frac{\partial(Au)}{\partial x} &= 0 \\
 P &= P(\rho, T), \quad P = P(\rho, e)
 \end{aligned}
 \tag{1}$$

LS-DYNA user input
Contours of Pressure
min=-262.245, at element 4230
max=272.17, at element 376691



Finite Levels
2.501e-01
2.413e-01
1.844e-01
1.276e-01
7.081e-02
1.406e-02
4.281e-02
-8.962e-02
-1.564e-01
-2.132e-01
-2.781e-01

LS-DYNA user input
Contours of Effective Strain (v) (v)
min=0.00000, at element 25801
max=10.0077, at element 25802



Finite Levels
1.500e+01
9.883e+00
8.879e+00
7.875e+00
6.871e+00
5.867e+00
4.863e+00
3.859e+00
2.855e+00
1.851e+00
6.079e-01

Figure 1. Contours of pressure of blast shock wave Figure 2. Progressive collapse of isolated structure under blast load

Secondly, the damage of the isolated structure in the near fault area has been studied. An analysis model of the LRB isolation structure is derived to analyze the dynamic response characteristics of isolation structure under near-fault ground motion. A secondary development program UACTIVE for the living and death of elements is compiled. In order to realize the failure simulation of the isolation bearing, the element linked to the isolation bearing spring is killed according to the maximum shear or axial force reaches a threshold value corresponding to the failure of isolation bearings.

$$\alpha = \frac{Q}{F}, \quad F = 1.0F_d + 0.25F_1 \quad (2)$$

where Q is the instability loading at different sector, and F is the loading combination specified by GSA2003.

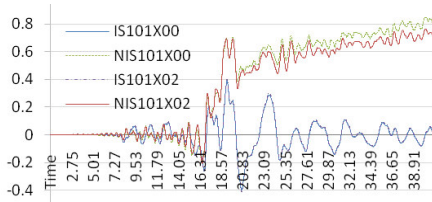


Figure 3 displacement X under Chichi-TCU101

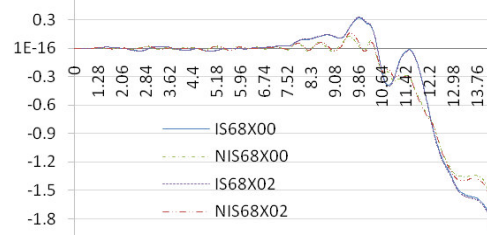


Figure 4 displacement X under Chichi-TCU068

Thirdly, the mechanism of vertical progressive collapse of the base-isolated structure and the effect of structural parameters on the mechanism are studied based on the same case of settlement, the comparative analysis of the settlement at different location and different parameters of isolation layer and different parameters of the super structure.

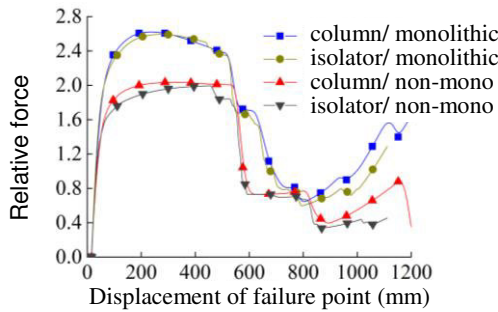


Figure 5 Pushdown curve with inner isolator removed

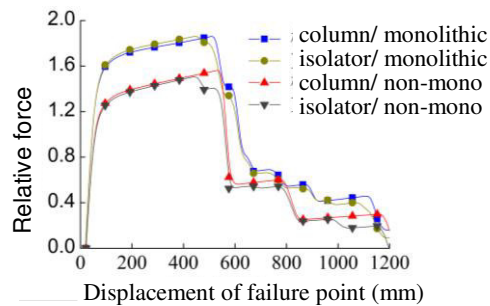


Figure 6 Pushdown curve with corner isolator removed

3. Conclusions

The results show that after the explosion in the basement of the isolated structure, the frame structure and the above-mentioned isolation bearing are directly destroyed, and the surrounding members have initial damage at different degree, which leads to the increased vertical deformation of the superstructure. A short lift effect is shown in the progressive collapse of isolated structure.

Isolated structure's displacement response and inter-story drift significantly increased in near-fault earthquake, with the most obvious characteristics being the large displacement in the underlying isolation layer, which may be the key reason for the damage of the isolated structure in near-fault region.

With the increase of fortification intensity, the progressive collapse resistance capacity is increased under the beam mechanism and catenary mechanism, but the increase under beam action is more obvious; Compared with the traditional structure, the failure of beam mechanism will be delayed in some conditions because of the constraints reduction in isolation layer.

EXPLORING THE ULTIMATE BEHAVIOR OF FRICTION PENDULUM ISOLATED STRUCTURES

Yu BAO

PhD Candidate, McMaster University, Canada
baoy7@mcmaster.ca

Tracy C. BECKER

Assistant Professor, McMaster University, Canada
tbecker@mcmaster.ca

Takayuki SONE

Chief Researcher, Takenaka Research and Development Institute, Japan
sone.takayuki@takenaka.co.jp

Keywords: Isolation; friction pendulum; impact; failure; shake table

Objectives

While it is well known that isolators provide enhanced seismic performance to structures under design basis ground motions, excessive displacements in large earthquakes are a potential issue for the safety of the isolated superstructure. Little dynamic study has been done on friction pendulum bearings, and the effects on the surrounding super structure. Sliding isolation bearings consist of one or more sliders with friction liners and corresponding concave sliding plates. Often there is a restraining rim along the perimeter of the sliding plate to prevent the slider from exceeding the displacement capacity.

This talk will present an experimental study on the extreme behavior of double friction pendulum bearings with the intent of better understanding the margin of safety available in designs. Four sets of sliding isolation bearings all with identical friction coefficient, sliding radius, and displacement capacity were tested on the shake table at the Applied Dynamics Laboratory at McMaster University, the experimental setup is shown in Figure 1. Each set of bearings had a different restraining rim design, representative of sliding bearings in Europe, Japan and the United States.

Afterwards, information on failure mechanisms and transmitted forces is used in numerical study focusing on best design methodologies for moment and braced frame buildings designed using these devices. A comprehensive numerical model is developed to incorporate both bearing failure and inelastic superstructure behavior. The former failure mechanism has been ignored in studies by previous research. A major consideration in this study is the effects of superstructure stiffness and yielding on the collapse performance. To this end, three base-isolated moment-resisting frames and concentric braced frames are designed in accordance with latest ASCE 7 code, representing code-compliant systems and systems where the superstructure is design to remain elastic. Fourteen pairs of near-fault pulse-like ground motions are used for collapse risk assessment.

Relevant Results

For the testing, the east-west component of the 1995 Kobe Takatori record was selected as the input ground motion because of its strong pulse component. The ground motion was scaled up until minor impact occurred; afterwards the ground motions were scaled up significantly larger so that incremental damage would not effect bearing behaviour. Bearing A, with no restraining rim, represents friction pendulum designs in Europe. For this bearing, no impact force could be transmitted as there was no restraining rim. However, the bearing failed (the interior slider dropped out) at 155% of the ground motion. Bearings C and D with rims, representing the North American design, experienced large impacts with forces of 1.5 to 2 g under the 155% ground motion. However, both Bearings C and D were functional after the impact when aftershocks of 80% Takatori were run. Bearings A and D are shown post-testing in Figure 2.

While Bearing A did eventually drop, it performed significantly better than expected. It was hypothesized that when the bearing had moved the so that the top and bottom plates each rested on only half of the interior slider (no overlapping area), the bearing would fall. However, because of the inertial restoring force, the bearing repeatedly remained stable after reaching this condition. While this is good for the overall stability of the system, it did cause

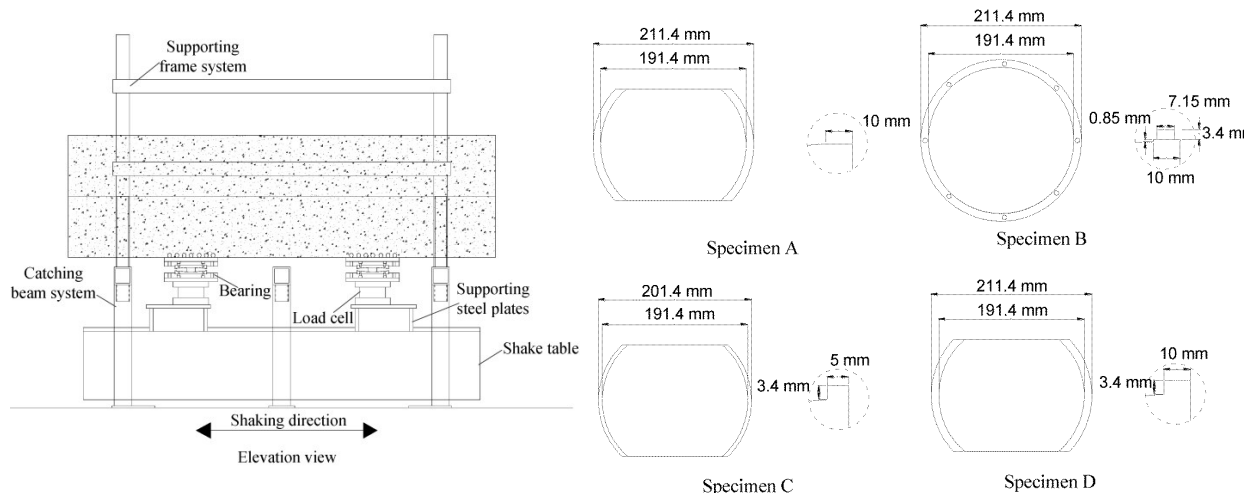


Figure 1: (left) Experimental setup, (right) bearing specimen



Figure 2: (left) Damage to Bearing set A (right) Damage to bearing set B

significant damage to the inner slider, which experienced shear forces during its return, scraping off the sliding liner. However, this would be acceptable damage in an extremely large event.

Bearings C and D differed in the thickness of their restraining rims. Bearing D, which had a thicker rim showed significantly less damage after the 155% ground motion. Bearing D transmitted a 15% higher impact force. Both bearings had large uplift and vertical accelerations caused from the impacts with the restrainer rims which was not present with Bearing A. The forces transmitted in the experimental tests of Bearings C and D were used to verify a numerical model of the bearings used at the base of the three-story moment and braced frames.

For the base-isolated moment-resisting frame, varying the design has a profound influence on its system-level failure mode. For the code compliant design and stronger frame design, the system-level failure mode is mixed: caused both by bearing failure and superstructure yielding. But for the larger bearing design, system-level failure mode is dominated by superstructure yielding. These changes indicate for flexible superstructure, increasing the superstructure strength has considerable beneficial effects on improving post-impact performance.

For the concentrically-braced frame, changing the design had a very limited effect on its system-level failure mode and total collapse risk. It is concluded for the stiff superstructure, impact force will impose substantial ductility demand on the superstructure regardless of its strength, therefore, the system-level failure solely comes from the superstructure collapse and only increasing bearing displacement capacity can improve its seismic performance. This observation also suggests for base-isolated stiff superstructure the impact should be avoided.

Conclusions

While the authors are still conducting studies comparing collapse margin ratio with and without restraining rims, the combination of experimental and numerical test suggest that the most resilient system is a strong but flexible superstructure placed on friction pendulum bearings with rims. This is because without rims the system will most certainly meet failure from excessive displacements. However, with the restraining rims, large forces will be transmitted to the superstructure. Ideally the superstructure will remain elastic, but if it does yield, a more flexible system will help control the ductility demands of the system.